IOP Publishing Journal of Physics B: Atomic, Molecular and Optical Physics

J. Phys. B: At. Mol. Opt. Phys. **40** (2007) 4617–4624 doi:10.1088/0953-4075/40/24/006

Model calculations of photoemission from a surface-deposited fullerene monolayer

O Kidun[1], D Bauer[1], N Fominykh[2] and J Berakdar[3]

[1] Max-Planck-Institut für Kernphysik, Postfach 10 39 80, 69029 Heidelberg, Germany
[2] Max-Planck Institut für Mikrostrukturphysik, Weinberg 2, 06120 Halle, Germany
[3] Insitut für Physik, Martin-Luther-Universität Halle-Wittenberg, Heinrich-Damerow-Str. 4, 06120 Halle, Germany

Received 3 September 2007, in final form 18 October 2007
Published 19 November 2007
Online at stacks.iop.org/JPhysB/40/4617

Abstract

We theoretically investigate the energy and the angular-resolved cross section for the photoelectron emission from a hexagonal monolayer of a C_{60} fullerene physisorbed on an inert substrate. On the basis of a tight-binding scheme with an on-site shell model for the single molecules we evaluate the energy and angular spectra of the photoelectrons upon the absorption of VUV linearly polarized photons. A symmetry analysis provides a clear interpretation of the observed structures in the numerically calculated cross sections. When the photoelectron is temporarily captured within the molecular cage, the symmetry of the angular emission pattern is mainly determined by the symmetry of the single fullerene molecule. In contrast, for the photoelectron state mainly located outside the C_{60} the angular dependence of the photoemission reproduces the symmetry of the lattice. These changes of the angular patterns repeat concurrently with the oscillations of the angle-integrated cross section.

(Some figures in this article are in colour only in the electronic version)

1. Introduction

The energy spectra of photo-emitted electrons from valence-band states of a single fullerene molecule C_{60} exhibit remarkable intensity oscillations [1, 2]. Existing theories [2–7] explain the nature of these oscillations by interference of photoelectron waves originating from the ionic sites. Similar intensity modulations are also observed for crystalline [10] and surface-deposited C_{60} layers [3, 8, 9] in which case the photoelectron spectrum also carries the signature of interferences of waves scattered from different crystal planes. A key point in the study of extended systems is the distinction between long-range (crystalline) and one-site (molecular) effects [11]. Indeed, it has been argued in a recent study on valence band by angle-resolved photoemission spectroscopy (ARPES) [12] of a C_{60} crystal that the photoemission angular anisotropy can be attributed to the intramolecular scattering of the photoelectron. The aim of

the present work is to investigate the manifestation of the long-range and short-range order in the photoelectron angular distributions and to reveal the connection of the photoelectron angular patterns with the oscillations in the angular-integrated spectra.

Generally, a characteristic length of the sample results in a characteristic momentum of the emitted photoelectron which shows up as a maximum of the photoemission probability as a function of the photon (or photoelectron) energy. An established example of this phenomenon is the oscillations in the extended x-ray absorption fine structure (EXAFS) of crystal solids. Multiple scatterings of the photoelectron wave from the ionic sites (where the potential is rapidly changing) lead to standing wave formation within some spatial domain. Qualitatively, the same picture is applicable to a fullerene film with the additional feature that the standing waves may also localize within molecular cages. The relatively large size of the fullerene forming the lattice as compared to ions forming atomic crystals is exhibited in two ways. Firstly, non-dipole effects may become visible, since the dipole approximation for the photon field is less justified[4]. Secondly, EXAFS 'decoding' (via Fourier transform) is most straightforwardly performed when the emitted photoelectrons are describable in terms of plane waves. In our case of the large characteristic length of the ionized system (due to the large radius of the fullerene), scattering eigenstates must be employed which in turn means an EXAFS-type interpretation [7] of the spectra should be revisited, as outlined below.

Generally, a maximum on top of an otherwise flat cross section (CS) can be viewed as a transition from a bound to a continuum-embedded *resonant* state. The latter state originates from constructive interferences between the outgoing photoelectron wave and the wave which is back-reflected from the potential. Such a quasistationary state differs from non-resonant continuum states by a stronger spatial localization and temporal delay (quantified by the variation of the phase shift with energy, the 'Wigner time'). Here we trace the footprints of the lattice periodicity and the length scale of the buckyball in the formation of the resonant states and their manifestation in the photoemission CS.

2. Theoretical framework

Deposited on inert surfaces such as graphite or SiO_2, fullerene molecules form hexagonal overlayers weakly bound to the substrate. The electronic properties of this superlattice are largely dominated by intermolecular interactions [13]. The substrate lattice structure underlies the crystal structure of the overlayer. We study the case where a linearly polarized electromagnetic wave (e_z is the polarization vector) impinges onto a fullerene monolayer film formed in the xy-plane. The lattice of C_{60} molecules has a six-fold symmetry and its unit cell is defined by the unit vectors $(1, 0)$ and $\left(\frac{1}{2}, \frac{\sqrt{3}}{2}\right)$. Three specific lengths characterize the film: the lattice parameter a, the radius of the fullerene molecule R and the averaged C–C chemical bond length δ. The potential of the C_{60} can be modelled by a spherically symmetric, shifted square well of width δ [4 , 14–16]. The external well radius coincides with the fullerene radius $R = 3.55$ Å. The width of the well reproduces the distance between neighbouring carbon nuclei $\delta = 1.42$ Å on the fullerene shell, and the potential depth is chosen such that 240 valence electrons are accommodated. We calculate the molecular wavefunctions in the Hartree–Fock approximation, accounting thus for the mean-field and exchange correlation between all valence electrons [17], but neglecting charge-correlation effects. The lattice parameter of the fullerene film is chosen $a = 10.02$ Å. Thus, the essential characteristics

[4] For the dipole approximation to be valid $k_\omega D \ll 1$ must apply, where D is the spatial extension of the electronic state and k_ω is the photon wave vector. For C_{60}, $D \approx 13.3$. Since the photon energy $E_\omega = \hbar\omega = \hbar k_\omega c$ we deduce $D\omega/c = \frac{13.3}{137}\omega \ll 1$, which sets the photon energy as $\omega \ll 10.3$ Hr ≈ 280 eV ($c = 137$ is light velocity).

of the sample are incorporated in the model via the shell structure and periodicity. Our hypothesis is that the angular distribution (AD) from such a system will switch between the molecule-like to the crystal-like shape concurrently with the oscillations in the angle-integrated photoionization cross section.

The van der Waals interaction between the deposited molecules splits each degenerate energy level of the single molecule into a narrow energy band, affecting the dispersion of the electron energy $E = E(\mathbf{q})$ ($\mathbf{q}$ is the electron's wave vector). A semi-empirical tight-binding (TB) model [18] accounts for this effect. In this approach, the electron localized on a given molecule is influenced by other molecules through a small correction (caused by van der Waals forces) to the potential at the chosen lattice site. The weakness of the van der Waals interaction as compared to the intermolecular forces naturally leads to a TB scheme which is adopted below. In what follows we calculate the photoemission CS from constant-energy initial states of the C_{60} film analogous to the constant initial state photoionization mode for a single molecule. Within the TB model and for our lattice the dispersion acquires the form

$$E(\mathbf{q}) = E_0 - A - 2\sum_{\alpha\beta\neq 0} B_{\alpha\beta}\cos \mathbf{q}\mathbf{a}_{\alpha\beta}. \tag{1}$$

Here E_0 is the energy of the molecular state generating the given band of the film. The TB parameters A and $B_{\alpha\beta}$ depend on the overlap of the molecular wavefunctions $\phi(\mathbf{r})$ located at the different sites. For the present calculations we find $A = -B_{\alpha\beta} \approx 0.004$, as inferred from the relation

$$A = \int_{R^3} |\phi(\mathbf{r})|^2 \Delta V(\mathbf{r})\, \mathrm{d}^3 r \tag{2}$$

$$B_{\alpha\beta} = \int_{R^3} \phi^*(\mathbf{r}) \Delta V(\mathbf{r}) \phi(\mathbf{r} - \mathbf{a}_{\alpha\beta})\, \mathrm{d}^3 r. \tag{3}$$

$\Delta V(\mathbf{r})$ derives from the one-site (H_{site}) and the lattice hamiltonian (H_{lattice}) as $\Delta V = H_{\mathrm{lattice}} - H_{\mathrm{site}}$. The strong on-site localization of the molecular wavefunctions restricts the summation over Miller lattice indices α and β to nearest-neighbour molecules and we end up with

$$E(\mathbf{q}) = E_0 - A - 2B\big(\cos q_x a + 2\cos \tfrac{1}{2} q_x a \cos \tfrac{\sqrt{3}}{2} q_y a\big). \tag{4}$$

3. Numerical results

Figure 1(a) shows the photoionization CS as a function of the photoelectron energy, calculated for a constant initial state of the single C_{60} molecule and for the monolayer film (figure 1(b)). For a comparison of the numerical results with available experimental data the highest occupied molecular orbital of C_{60} was chosen as the initial state. Open circles denote the experimental CS values obtained for C_{60} in the gas phase [2]. The ionization rate of the film is calculated for two bands developing from the highest (HOMO) or from the lowest (LOMO) occupied valence molecular orbital of free fullerene[5]. The constant initial state of the film was chosen at the bottom (Γ-point, $\mathbf{q} = 0$) of the dispersing band. The Fourier transforms of the cross section $\sigma(k)$ (with $k = \sqrt{\omega + \epsilon_{\mathrm{ini}}}$ the photoelectron wave vector) are plotted in the insets in figure 1. As the photoelectron energy is not large enough to apply the plane wave description

[5] The valence lowest molecular state of a_g symmetry represents the physical counterpart of the LOMO in the spherical shell model.

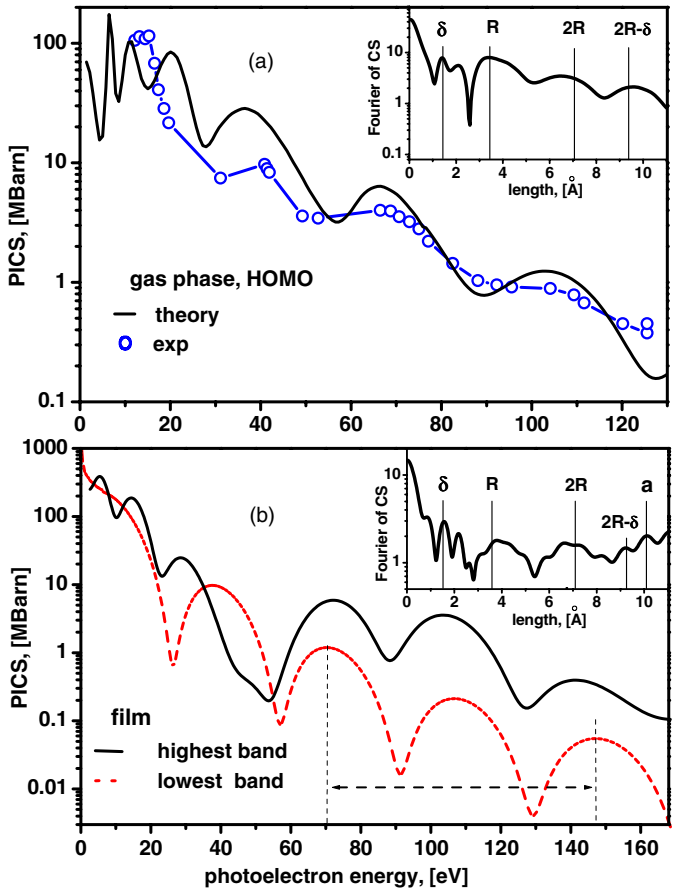

Figure 1. The ionization CS (a) of the single fullerene, and (b) of the monolayer film as a function of the photoelectron energy. The HOMO of the free C_{60} (a, black curve), the bottom of the highest (b, black curve) and of the lowest (b, red curve) occupied bands of the film were chosen as the initial. The experimental data [2] are shown by open circles on figure a. The Fourier transforms (FT) of the HOMO-CSs are plotted in the corresponding insets. The spatial positions of the FT maxima approximately coincide with the main characteristic lengths (and their satellites) of the ionized system denoted by vertical lines: the fullerene radius R, the minimal internuclei distance δ, and the lattice parameter a.

of the final state, we use the numerically evaluated scattering states instead. Nevertheless, the spatial positions of the FT maxima of the CSs are very close to the values of the characteristic lengths and of their satellites, as indicated in the figure by vertical lines.

Now we turn to the investigation of the angular properties of the photoemission. For the calculation of the photoelectron angular distributions the electronic states of the LOMO-band were chosen as the initial state. The icosahedral group I_h is close to spherical symmetry, and the parentage of the low-lying molecular orbitals in spherical harmonics can be discerned. In particular, the S, P and D spherical harmonics become a_g, t_{1u} and h_g representations [19]. The 3D distribution of a lowest a_g molecular wavefunction is nearly spherical and, in a good approximation, can be modelled by the lowest S-state (LOMO) of the spherical shell model. The angular distribution of photoelectrons (ADP) for the free fullerene is governed by the initial state symmetry. In the given model for the molecular potential and for a linear

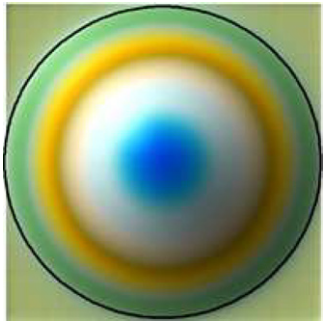

Figure 2. Stereographic projection of the photoelectron p-wave, oriented normally to the plane of the film.

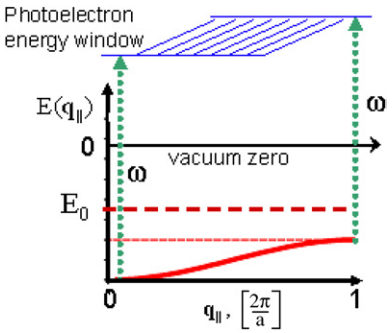

Figure 3. Schematic representation of the transition from the initial band (∼1 eV wide for the highest and ∼0.5 eV for the lowest occupied band) to the photoelectron energy window for a given photon energy ω.

photon polarization it obeys the dipole selection rules for the orbital momentum $\ell_f = \ell_0 \pm 1$ and for the magnetic quantum number $m_f = m_0$. For the ionization of the lowest energy state with zero orbital momentum the ADP is a p-wave aligned along the photon polarization vector e_z. Its stereographic projection onto the xy-plane has a single maximum in the direction perpendicular to the plane (figure 2). In the case of the periodical lattice the situation is totally different. When the energies of the photon ω and of the initial state $E(\mathbf{q})$ are fixed, the photoelectron energy $|\mathbf{k}|^2$ is uniquely determined by the conservation law $k^2 = \omega + E(\mathbf{q})$. The lattice periodicity leads to the conservation of the parallel momentum $\mathbf{k}_{||} = \mathbf{q}_{||} + \mathbf{G}_{\alpha\beta}$. Here $\mathbf{G}_{\alpha\beta}$ is the reciprocal lattice vector. Both rules prescribe the emission from a given initial state to fixed directions only. Therefore, if we are interested in the *angular* patterns we have to scan through the chosen initial band. For the allowed final states this scanning determines a certain energy window of the same width as the initial band (see figure 3). The ADPs calculated for the different photon frequencies are presented in figure 4 as a set of stereographic projections onto the plane of the film. On the left-hand side of each subplot the energy of the *photoelectron* state (which is taken at the bottom of the energy window of the final states (see figure 3)), is given. The range of photon energies is chosen as to span approximately two periods of the oscillations in the photoionization CS.

The symmetry of the ADP is determined by the six-fold symmetry of the lattice. Four main features of the angular patterns can be inferred from the calculated data.

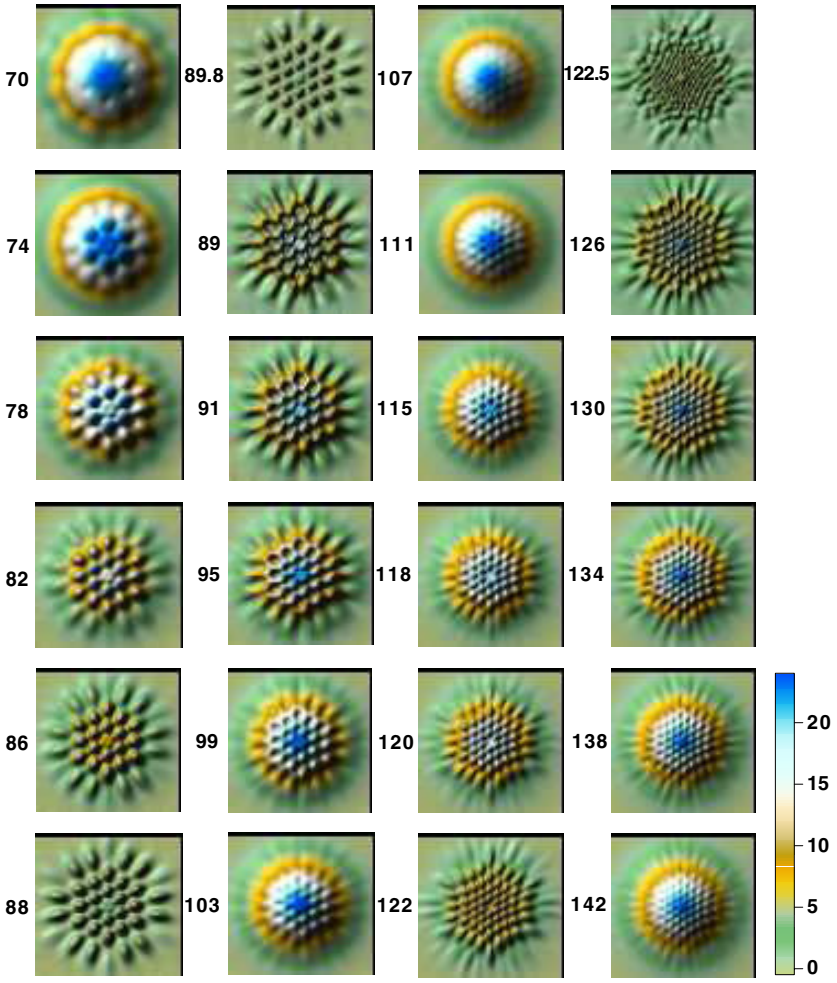

Figure 4. Set of stereographic projections of the ADP for different photon frequencies. The LOMO-band is chosen as a constant initial band. The energy range (it is depicted by the dashed arrowed line in figure 1(b) covers two periods of oscillations in the photoionization CS. The minimal value $k^2_{\min}$ of the photoelectron energy (in eV), i.e. of the electron ionized from the Γ-point of LOMO-band, is shown at the left hand side of each plot. The energies of other electrons contributing to a certain ADP are in the range $[k^2_{\min} \cdots k^2_{\min} + 0.5\ \text{eV}]$. For the explanation of the observed features see the discussion in the text.

(1) The first observation is that the shape of the ADPs is periodically repeated, along with the periodic oscillations in the CS (cf figure 1). We arranged our data set in four columns. The first two columns span one period of the oscillations of the CS (70–103 eV), the other two columns the next period (107–142 eV). Tracing the qualitative changes from the top to the bottom of each column, we note that the diffraction spots, reflecting the six-fold symmetry of the lattice, can become very sharp (as for the energies 88 eV or 122 eV), or very smeared out (as for the energies 70 eV or 107 eV). Moreover, the number of diffraction spots grows with increasing photoelectron energies, as seen for example at 95 eV and 134 eV (or any other pairs of plots in even (odd) columns in the same rows).

This is explained by the inclusion of next-order diffraction beams as the photon energy increases.

(2) At the photoelectron energies corresponding to the maxima in the ionization CS (70 eV and 107 eV) the angular patterns resemble the emission from the free molecule (cf figure 2). This is due to the resonant capture of the photoelectron inside the molecular cage where the influence of the surrounding molecules on the photocurrent is small. There the lattice is not dominating, and its influence is manifested only in the form of weak reflexes superimposed onto the main broad *p*-wave maximum.

(3) At the photoelectron energies 88.8 eV and 122.5 eV corresponding to the minima in the CS, the lattice symmetry is most pronounced because the photoelectron becomes delocalized in the film. In general, we observe a continuous evolution of the patterns, from the domination of the molecular shape to the lattice shape and back.

(4) Around certain photoelectron energies (cf the plots for 88.8 and 89 eV) a slight change in the photoelectron energy yields a sudden change of the preferable emission directions (minima and the maxima replace each other). This effect is determined by the change of the sign of the photoelectron scattering phase, which physically is responsible for the acceleration or deceleration of the particle in given directions. As a result, the photoelectron is emitted along or between the crystallographic directions. Such a profound switch in the focusing of the photoelectron is yet to be confirmed experimentally.

4. Conclusion

We investigated theoretically the energy and the angular properties of the photoelectron emission from a monolayer fullerene film, forming a hexagonal molecular lattice on an inert substrate. We find the angular distribution of the ionization probability experiences drastic modifications as a function of the photon energy. The angular-resolved spectrum manifests three general features. Firstly, its pattern repeats with the oscillations in the photoionization cross section. Next, when the photoelectron is temporarily captured within the molecular cage, the symmetry of its angular emission is mainly determined by the symmetry of the single molecule. In contrast, for the photoelectron state mainly located outside the C_{60} (where the CS shows local minima) the angular dependence of the emission reproduces the symmetry of the lattice. In the vicinity of the CS minima there exist narrow photon energy intervals $\sim$0.1 eV, where the preferable directions of photoemission undergo sudden changes.

References

[1] Liebsch T *et al* 1995 *Phys. Rev.* A **52** 457
[2] Xu Y B, Tan M Q and Becker U 1996 *Phys. Rev. Lett.* **76** 3538
[3] Hasegawa S J *et al* 1998 *Phys. Rev.* B **58** 4927
[4] Frank O and Rost J M 1997 *Chem. Phys. Lett.* **271** 367
[5] Rüdel A *et al* 2002 *Phys. Rev. Lett.* **89** 125503
[6] Kidun O, Fominykh N and Berakdar J 2005 *Chem. Phys. Lett.* **410** 293
Kidun O, Fominykh N and Berakdar J 2004 *J. Phys. B: At. Mol. Opt. Phys.* **37** L321
[7] Kidun O, Fominykh N and Berakdar J 2006 *Comput. Math. Sci.* **35** 354
[8] Benning P J *et al* 1991 *Phys. Rev.* B **44** 1962
[9] Ton-That C *et al* 2003 *Phys. Rev.* B **67** 155415
[10] Wu J *et al* 1992 *Physica* C **197** 251
[11] Molodtsov S L *et al* 1992 *Europhys. Lett.* **19** 369
[12] He S *et al* 2007 *J. Phys.: Condens. Matter* **19** 026202
[13] Maxwell A J *et al* 1998 *Phys. Rev.* B **57** 7312
[14] Puska M J and Nieminen R M 1993 *Phys. Rev.* A **47** 1181

[15] Keller S and Engel E 1999 *Chem. Phys. Lett.* **299** 165
[16] Amusia M, Baltenkov A and Becker U 2000 *Phys. Rev.* A **62** 12701
[17] Kidun O and Berakdar J 2002 *Surf. Sci.* **507** 662
[18] Pettifor D G 1995 *Bonding and Structure of Molecules and Solids* (Oxford: Oxford University Press)
Sutton A P 1993 *Electronic Structure of Materials* (Oxford: Oxford University Press)
[19] Haddon R C, Brus L E and Raghavachari K 1986 *Chem. Phys. Lett.* **125** 459